Acquisition and processing of Troll apparition 3D streamer data

Sergio Grion(*), Lorenzo Casasanta(*), Simon Brown, Per Riste(**), Mike Cogan(**) and Lasse Amundsen (**)

(*): Shearwater GeoServices
(**): Equinor ASA

Abstract

This paper presents acquisition and processing results from a 3D streamer acquisition trial of triple-source apparition data, with an emphasis on processing. We show that, after apparition de-blending, initial migration results did not show resolution improvements over a reference unblended dual-source dataset. However, attentive 3D processing of the same de-blended data gave substantial improvements to image resolution. Time slices from the fully processed apparition data show higher resolution than the corresponding reference data.

Introduction

The rapid rise in the number of blended acquisition projects with multiple sources has been driven by the need for higher resolution and improved operational efficiency. De-blending schemes can either rely on random shot dithers or on periodic time delays and the apparition method (Amundsen et al.,2018). In seismic data apparition, multiple sources are activated almost simultaneously with periodic time delays of the order of milliseconds. This periodic encoding facilitates the separation of individual sources and provides increased fold and sampling with respect to conventional blended surveys. The objective of this paper is to present the acquisition of experimental apparition data over the Troll field and discuss 3D processing results for the apparition data and a reference dataset acquired for commercial surveying.

Acquisition

The apparition 3D survey was carried out in July 2019 over Troll, a producing oil and gas field located in the North Sea on the Norwegian continental shelf, and the commercial survey used as a reference was acquired shortly before the apparition test. The source configurations used are described below.

Survey	Source configuration	Inline sampling	Cross-line sampling
Reference	Dual 3147in^3, 4m depth	37.5m (18.75m flip-flop)	37.5m
Apparition	Triple 1049in^3, 4m depth	12.5m (12.5m simultaneous)	25m

For both surveys the record length was 5s and the streamer configuration was also the same, with 12 multi-component streamers 2.4km long and 75m apart, deployed at 15m depth. The apparition test consisted of 7 lines 437.5m apart and 10km long, resulting in 30km^2 of 3D data.
Seven lines close to the apparition lines were selected from the commercial survey, with the objective of comparing image quality from the reference and apparition data under the constraint of equal acquisition cost. The weather was fair during acquisition of the apparition data, with variable swell having a significant wave height of between 0.5 and 1m. The seven lines extracted from the commercial survey have similar noise level to the apparition lines.

The apparition time dithers used are described by the following time modulation matrix (in milliseconds):

$$Tmod = \begin{bmatrix} 0 & 7 & 22 \\ 7 & 22 & 0 \\ 22 & 0 & 7 \end{bmatrix} \qquad (1)$$

where rows indicate successive shot points and columns indicate the starboard, central and port sources, from left to right. For triple-sources, the modulation codes repeat every three shots. This choice of modulation codes ensured minimal sensitivity to noise in the 3-100Hz band (Figure 1). The optimisation of modulation codes used here is described in Grion et al., 2018. To summarise, apparition de-blending can be achieved by inverting a linear system of equations, and any such inversion has an associated sensitivity to noise that can be quantified by calculating the posterior noise standard deviation (Tarantola 2005).

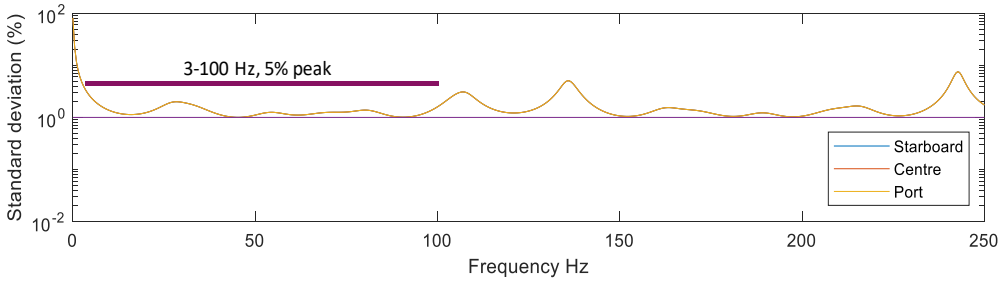

***Figure 1**: Posterior standard deviation of apparition de-blending for the modulation codes in equation (1), as a percentage of prior standard deviation. The chosen modulation codes ensure that de-blending into port, starboard and centre sources has the same posterior deviation.*

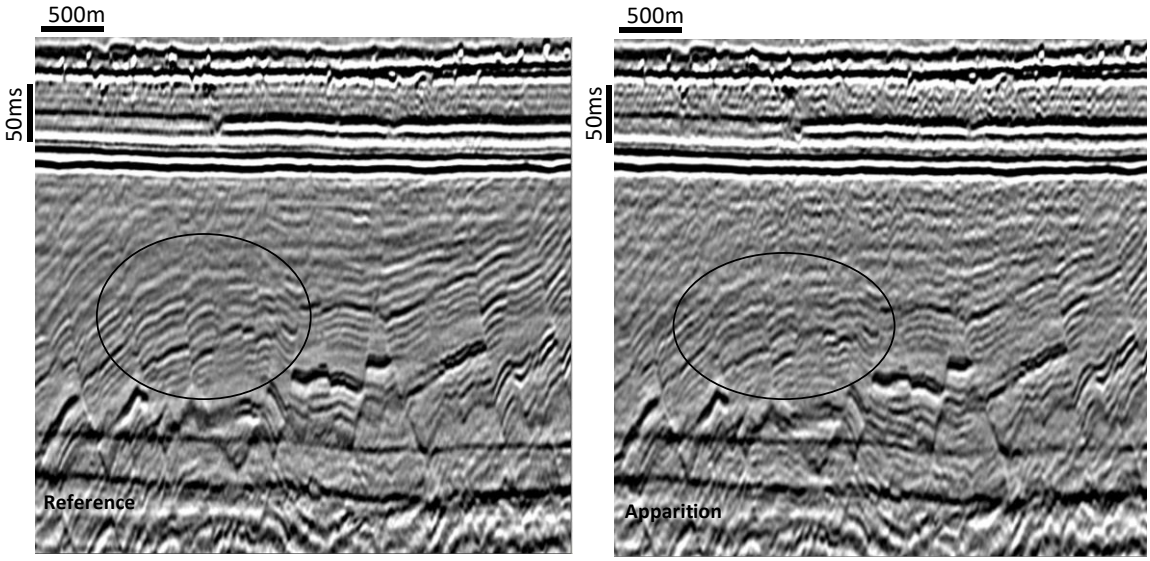

Figure 2 *Initial Reference and apparition 3D PSTM. In the tilted fault blocks area highlighted, the reference dataset shows better focusing despite having 3 times less fold.*

Processing

On-board processing dealt with occurrences of seismic interference, swell noise, cable bend noise, propeller noise and rig reflection noise. All these noise types were effectively removed. After receiver motion correction, the dense hydrophone and accelerometer data was then processed for wavefield separation, to deliver up-going pressure data sampled at 6.25m along each of the 12 cables. It is interesting to point out that the apparition data, because of the short delays (milliseconds) between the blended sources, could be de-ghosted onboard, before office-based de-blending. Blended surveys with random dithers typically use delays of the order of seconds and this requires special consideration in de-ghosting, as methods with long impulse responses are unsuitable for application before de-blending.

For both reference and apparition data, de-signature was carried out using an average, NFH-derived operator. Since the NFH data is blended in the apparition case, the far-field signatures were de-blended before averaging. Casasanta et al. 2020 describe a shot-by-shot de-signature procedure for apparition data, but this was not used for the processing results shown here. For the purpose of this study, apparition de-blending of the upgoing wavefield was carried out using the method of Andersson et al. 2017 and provided to us by its authors. A comparison of initial 3D migrated target lines for the reference and de-blended apparition data is shown in Figure 2. These images were obtained without any further processing, to assess whether the de-blended apparition data showed higher resolution than the reference at this early processing stage. A comparison of the two images in a challenging area with tilted fault blocks unfortunately revealed better resolution and SNR for the reference data, a sign that the apparition data is affected by noise, probably residual blending noise. We then planned for a full 3D processing sequence of both datasets in order to further investigate resolution issues.

Multiple attenuation was carried out using 3D SRME followed by the application of Radon filters. The increased shot sampling has potential for improved SRME results but careful QC both of predicted models and post adaptive subtraction could not identify better de-multiple results for the apparition data. However, it is important to note that apparition and reference lines are not coincident and subtle improvements would not be identifiable form the inspection of target lines. Although the apparition data has better sampled Radon gathers, the resilience to aliasing of the high-resolution Radon allowed for similar reference and apparition results to be achieved. We note that Radon filters played a role in reducing residual blending noise on the apparition data.

Both reference and apparition common offset volumes were then individually regularized to their nominal binning geometry along three spatial dimensions (the inline and cross-line coordinates of bins, and offset). The resulting apparition volume has three times the fold of the reference volume.

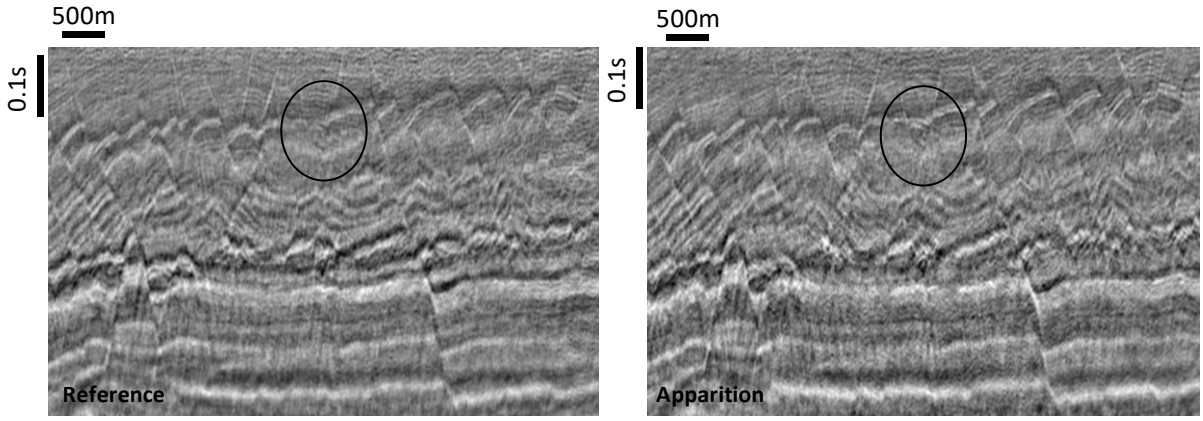

Figure 3 *Final Reference and apparition 3D PSTM. The apparition and reference images are of similar quality, but apparition is occasionally slightly better (see highlighted area).*

A comparison of target lines migration after full processing shows that the apparition and reference data now have similar resolution. This is consistently achieved with apparition data, as noted for example by Casasanta et al. (2019). We then investigated AVO attributes for the target lines but found similar quality of fit for the two datasets, although intercept and gradient are in general better for the apparition data in the shallow part of the section, where the fold of the reference data is particularly low. On the other hand, the inspection of time slices clearly shows the superiority of the apparition result. The shallow targets allowed 3D migration of the 30km^2 dataset to an8.5km by 2km image, down to 5s (Figure 4). We inspected time slices down to 1s ad found the apparition data consistently better.

Conclusions

This study demonstrates that the fold and illumination advantages of apparition data can lead to better quality images. Given the careful design and the many years of acquisition and processing research on conventional data, the reference data image is quite detailed, but the apparition data image is even better, in areas with complex structures. Apparition data processing needs to preserve this additional resolution throughout the processing sequence, for image improvements to be substantial. We point out that an initial 3D migration of a target inline post de-blending but with no other processing applied resulted in an apparition image with slightly less detail and more noise than the reference image. This was later reversed through attentive 3D processing of both datasets.

Acknowledgements

The authors are grateful to Equinor ASA and Troll license partners for permission to show the Troll data example, to Seismic Apparition GmbH for providing the de-blended data and to the crew of the Amazon Conqueror for their efforts during the acquisition and on-board processing of the apparition data.

References

Amundsen L., Andersson F., van Manen D.-J., Robertsson J.O.A., and Eggenberger K. [2018], Multisource encoding and decoding using the signal apparition technique. Geophysics 83, V49–V59.
Andersson, F., van Manen, D. J., Robertsson, J. O. A., Wittsten, J., and Eggenberger, K. [2017], Analytic dealiasing in seismic apparition. *79th EAGE Conference & Exhibition, Extended Abstracts*
Casasanta, S., Grion, S., Martin D. and Denny, S. [2019], Evaluation of streamer apparition processing results, *81st EAGE Conference & Exhibition, Extended Abstracts*
Casasanta, L., Telling, R. and Grion, S. [2020], De-signature of apparition-blended seismic data: a North Sea example. *SEG Technical Program Expanded Abstracts*, 2888-2892
Grion, S., Martin, D., and Denny, S. [2018] Modulation codes and data processing for seismic apparition of towed-streamer seismic data. *SEG Technical Program Expanded Abstracts*, 4201-4205
Tarantola, A., 2005, Inverse problem theory, SIAM

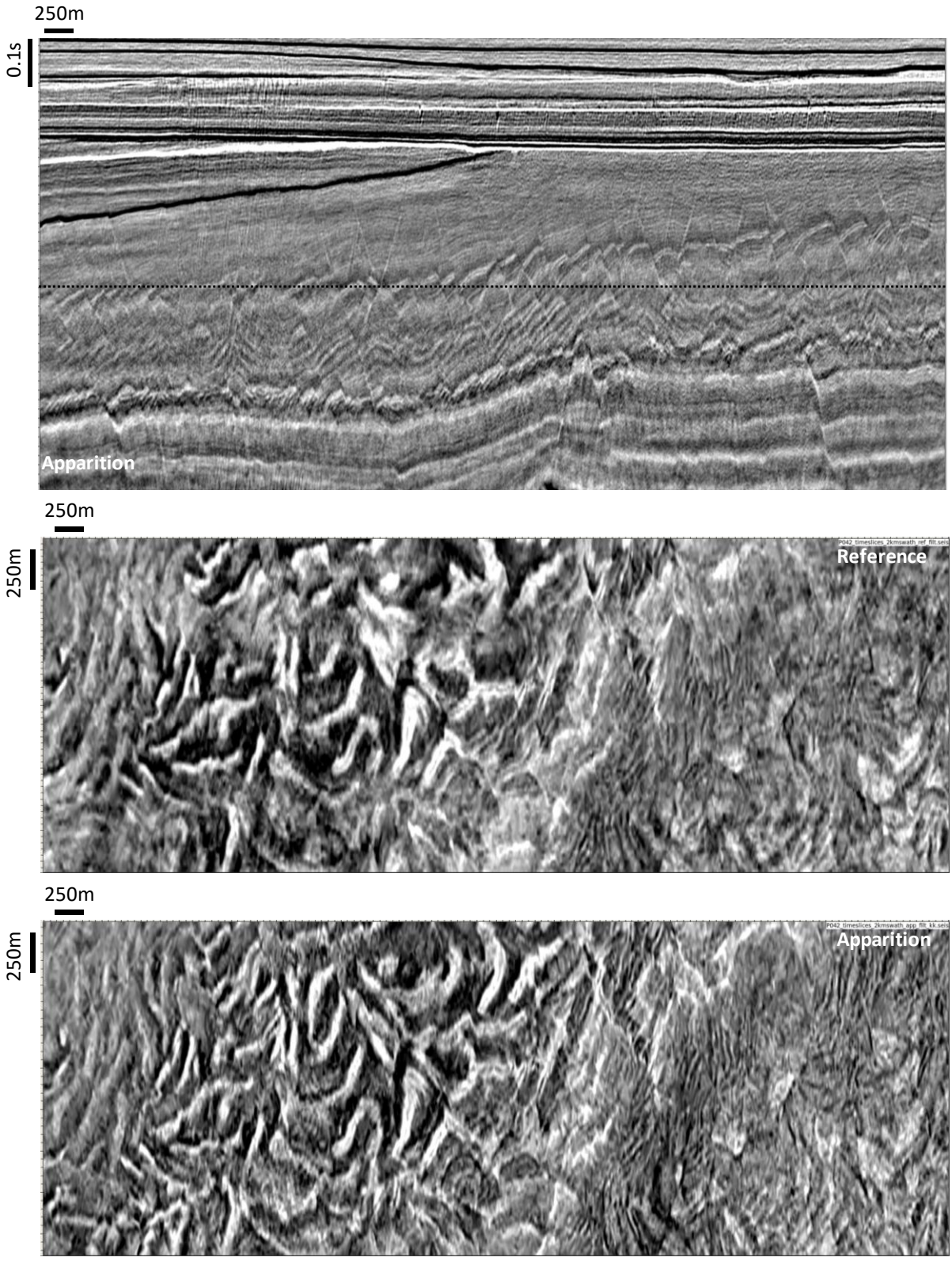

Figure 4 *Apparition PSTM image (top) and comparison of time slices at 960ms two-way-time for the reference and apparition data. After full processing, the apparition data shows higher resolution in the presence of complex structures. The slice level is indicated by a dashed line.*